Soil Dynamics and Earthquake Engineering 104 (2018) 372–377

Contents lists available at ScienceDirect

Soil Dynamics and Earthquake Engineering

journal homepage: www.elsevier.com/locate/soildyn

Liquefaction resistance of fibre reinforced low-plasticity silt

Amin Chegenizadeh*, Mahdi Keramatikerman, Hamid Nikraz

Department of Civil Engineering, Curtin University of Technology, Kent Street, Bentley, Perth, Western Australia 6102, Australia

ARTICLE INFO

Keywords:
Low plasticity silt
Liquefaction resistance
Cyclic triaxial
Fibre

ABSTRACT

This study sought to investigate the effect of bulk continuous filament (BCF) on the liquefaction resistance of low plasticity silt by performing a series of cyclic triaxial tests on the reference (unreinforced) and reinforced specimens. The effects of BCF contents and length (*BL*), relative density (D_r), and effective confining pressure (σ'_3) on the liquefaction strength of the reinforced specimens were investigated and the results were compared with the reference tests. The results showed that increasing the BCF content improved the liquefaction resistance of the silt. Also, it was noted that increasing the fibre length from 5-mm, to 10-mm and 15-mm respectively, increased the liquefaction resistance of the specimens. The results in the next stage showed that by increasing the relative density (D_r), liquefaction resistance of a reinforced specimen is more pronounced than that of an unreinforced specimen. Finally, investigations on the effect of effective confining pressure (σ'_3) on the liquefaction resistance of the reinforced specimens showed that increasing the effective confining pressure reduced the liquefaction resistance of the specimens due to suppression of the dilatancy.

1. Introduction

Silt is known as a fine-grained soil that is vulnerable to liquefaction during the event of an earthquake [1]. Primarily, Seed et al. [2] noted that a fine-grained soil requires the fulfilment of three conditions in order to be counted as a non-liquefiable soil, based on the Chinese criteria. The constraints involve factors such as having a fines content less than fifteen percent, a liquid limit (*LL*) less than thirty-five percent and a water content (W_c) higher than ninety percent of liquid limit. The liquefaction assessment using Chinese criteria was later challenged by observation of some examples of liquefaction in silty and clayey soils [3]. Some other studies highlighted the importance of the plasticity index (*PI*) as a more crucial set of parameters in studies of fine-grained soil [4–8].

Boulanger and Idriss [9] also discouraged the use of Chinese criteria in the liquefaction investigation of a fine-grained soil and studied mechanical criteria in the liquefaction susceptibility of fine-grained soils. They recognised two groups of the clay-like (when $7 \leq PI$ and $5 \leq PI$ in *CL-ML* soils) and sand-like soils in studying the cyclic behaviour of fine-grained soils and proposed using the term “cyclic softening failure” instead of “liquefaction” for fine-grained soil with clay-like behaviour. El Takch et al. [10] also studied the cyclic behaviour of a silt and a sandy silt soil and reported that non-plastic silts are susceptible to liquefaction and they behave similarly to sand in terms of excess pore water generation and strain. They also indicated that the cyclic stress ratio (*CRR*) of the soil increased with the increase of silt content at the same void ratio.

Application of fibre in ground improvement originated from the reinforced soils by the roots of trees. Many studies have been performed to investigate the effect of the fibre reinforcement. For instance, Boominathan and Hari [11] investigated the effect of fibre reinforcement on the liquefaction strength of fly ash. They indicated that the addition of fibre increased the liquefaction resistance of fly ash due to the provision of interlocking behaviour and dissipating excess pore water pressure amongst fly ash particles.

In another case, Noorzad and Amini [12] investigated the effect of fibre reinforcement on the cyclic strength of silty sand and reported that the addition of fibre reduced the liquefaction susceptibility of the soil. They also indicated that reinforcement is more effective in specimens with medium density than in loose samples [12]. In another study, Vercueil et al. [13] investigated the effect of the addition of woven and non-woven geosynthetics with different mechanical characteristics to the sand and reported that the cyclic strength of the soil increased when geotextiles were included in the sand. Maher and Ho [14] investigated the behaviour of fibre-reinforced cemented sand under cyclic loading. The results indicated that the addition of fibre improved the cyclic strength of the cemented sand.

The liquefaction vulnerability of the fine-grained soil was discussed in the aforementioned literature and it was proven that low plasticity silt is a type of fine-grained soil that is prone to liquefaction, and has a behaviour similar to that of coarse-grained soils such as sand. Also, according to the literature, it was noted that fibre reinforcement is an

* Corresponding author.
E-mail addresses: amin.chegenizadeh@curtin.edu.au (A. Chegenizadeh), mahdi.keramatikerman@postgrad.curtin.edu.au (M. Keramatikerman), h.nikraz@curtin.edu.au (H. Nikraz).

https://doi.org/10.1016/j.soildyn.2017.11.004
Received 26 September 2016; Received in revised form 23 August 2017; Accepted 4 November 2017
0267-7261/

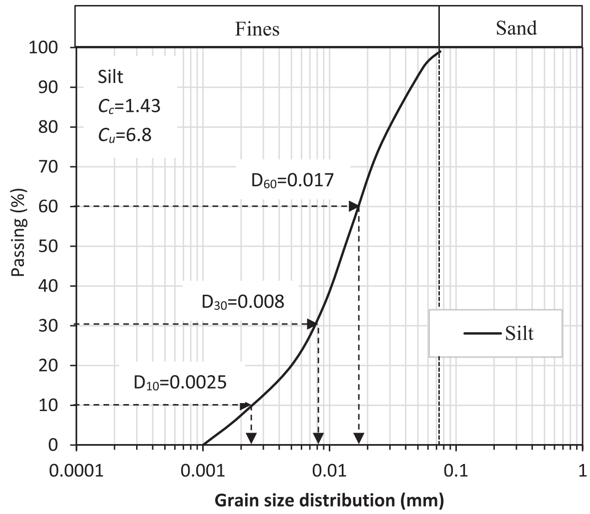

Fig. 1. Particle size distribution (PSD) of the used silt.

accepted approach in liquefaction mitigation. Therefore, this study investigates the fibre reinforcement of low plasticity silt. This research is in continue of the Liquefaction study [15] at Curtin University.

2. Test materials

The silt used for this study was sourced from Canning River, Perth, Western Australia. The particle size analysis conducted on the low-plasticity silt and the results were presented in Fig. 1 (ASTM D4221 [16]). The analysis showed that the used silt has a coefficient of uniformity (C_u) and a coefficient of curvature (C_c) of 6.8 and 1.43 respectively. Also, the particle size distribution (PSD) analysis showed that this soil has a mean grain size (D_{50}) of 0.014 mm, and a D_{10} and D_{60} equal to 0.0025 and 0.017-mm respectively. The index properties tests were performed according to ASTM D4318 [17], and the results showed that the used silt has a liquid limit (*LL*) of 26%, plastic limit (*PL*) of 21.4%, and a plasticity index (*PI*) of 4.6%. The used silt is classified as the *ML* according to the Unified Soil Classification System (USCS) (ASTM D2487 [18]). The fibre used to reinforce the specimens is known as bulk continuous filament (BCF) fibre, and has a tensile strength, and an elastic modulus of 415 MPa and 3.12 GPa respectively. Also, the proportion of mass to length and the specific gravity was equal to 0.96 g/cm and 1.25 respectively. Fig. 2 presents a typical BCF used in this study.

3. Sample preparation

The “wet tamping” and the “slurry deposition” methods are two main sample preparation techniques in triaxial testing, and selection of each method would affect the results of the study [19]. During the testing phase, it was figured out that the wet tamping technique (i.e., under-compaction) works better, since in this method the uniformity of the reinforced specimens is maintained rightfully. In contrast with the wet tamping technique, the specimen is unable to stand alone during the trimming due to its inability to hold suction in the slurry deposition method [20]. The sample preparation using the under-compaction technique is a well-accepted and applicable method for silt as indicated by Ladd [21] and Prakash and Sandoval [8]. In this method, the lower layer becomes denser by compaction of the upper layer, and each layer becomes compacted to a lower density than the previously targeted. Therefore, the under-compaction rate of each layer linearly varies from the bottom to the top of the specimen, and the required under-compaction can be estimated [22]. Application of this fabrication technique helps the user to have good control of the density of each layer while the BCF is not segregated, and a situation similar to the real condition has been simulated for a reinforced specimen. In this study, specimens with uniform density and identical BCF distribution by moist tamping the silt mixture in 5 layers was obtained using the under-compaction technique. The cylindrical specimens with 120-mm height and 62.5-mm diameter were prepared for each test. To prepare the specimens initially, the silt was mixed with BCF and/or clay and thoroughly stirred. Then, a water content equal to 8% of the weight of the mixture was added to the mixture for ease of mixing, and thoroughly stirred [8,12]. The specimens were fabricated in three initial relative densities (D_r) of 40%, 60%, and 80%. Also, the recorded maximum and minimum relative density was of 0.76 and 0.52 respectively.

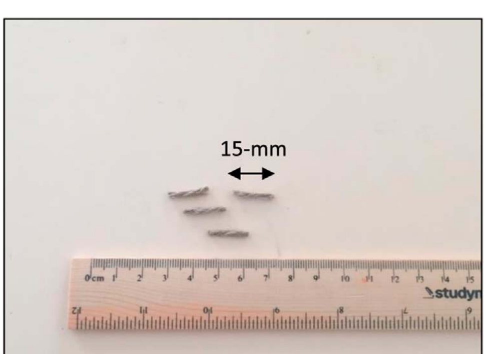

Fig. 2. Bulk continuous filament (BCF) cut in 5, 10, and 15-mm lengths.

4. Methodology

A series of stress-controlled cyclic triaxial tests were performed in accordance with ASTM D 5311 [23] to investigate the effect of BCF reinforcement on the silt specimens using a Geocomp cyclic triaxial apparatus. To conduct the tests, CO_2 gas was injected through the specimen for about one hour [22]. Then, the distilled and de-aired water was passed through the specimen using a low pressure. After that, the distilled and de-aired water was injected through the specimen using a minimum amount of 500-kPa back pressure. The saturation stage was then completed when the ratio of the pore water pressure (Δu) to the variation in cell pressure ($\Delta\sigma_c$), or simply B_{value}, was equal or greater than 0.95 ($0.95 \leq \Delta u/\Delta\sigma_c$). In the consolidation stage, the desired effective confining pressures (σ'_3) of 50, 100 and 150-kPa were applied to the specimens. The variations of the axial displacement and pore water pressure were recorded with a symmetrical sinusoidal pulse frequency of 0.5-Hz and cyclic stress ratio (*CSR*) of 0.18, 0.25 and 0.35 were selected according to Eq. (1).

$$CSR = \frac{(\sigma'_{max} - \sigma'_{min})}{2\sigma'_{min}} \tag{1}$$

where σ'_{max} = maximum principal effective stresses; and σ'_{min} = minimum principal effective stresses. Table 1 illustrates the experimental program which followed to conduct the tests. The post-consolidation relative densities ($D_{r,\ p}$) were recorded based on the pre-consolidation relative densities (D_r), and the occurred volumetric strain after the consolidation stage.

5. Results and discussion

5.1. Typical test results

A typical result of the cyclic triaxial test for a silt specimen reinforced with 0.3% BCF, and a post consolidation relative density ($D_{r,\ p}$) of 42.2% at a CSR value of 0.25 was shown in Fig. 3. It is seen from variation of the deviator stress versus number of cycle to liquefaction (q-N_L) that a harmonic loading pattern with ± 75-kPa of deviator stress (q) is applied to the specimen [see Fig. 3(a)]. This harmonic deviatoric

Table 1
Experimental program to investigate effect of the reinforcement on silt specimen.

No.	σ'_3 (kPa)	BCF (%)	BCF length (mm)	D_r (%)	$D_{r,\ p}$ (%)	*CSR*	N_L	*B*-value
	Effect of BCF content							
1	150	–	–	40	42.2	0.18	60	0.96
2	150	–	–	40	42.2	0.25	42	0.95
3	150	–	–	40	42.2	0.35	17	0.95
4	150	0.3	5	40	42.2	0.18	86	0.97
5	150	0.3	5	40	42.2	0.25	79	0.97
6	150	0.3	5	40	42.2	0.35	33	0.97
7	150	0.5	5	40	42.2	0.18	114	0.95
8	150	0.5	5	40	42.2	0.25	90	0.95
9	150	0.5	5	40	42.2	0.35	44	0.95
10	150	1	5	40	42.2	0.18	137	0.96
11	150	1	5	40	42.2	0.25	108	0.96
12	150	1	5	40	42.2	0.35	48	0.97
	Effect of BCF length							
13	150	0.3	10	40	42.2	0.18	105	0.97
14	150	0.3	10	40	42.2	0.25	93	0.95
15	150	0.3	10	40	42.2	0.35	42	0.95
16	150	0.3	15	40	42.2	0.18	139	0.96
17	150	0.3	15	40	42.2	0.25	107	0.96
18	150	0.3	15	40	42.2	0.35	47	0.95
	Effect of relative density							
19	150	–	–	60	64.1	0.18	81	0.96
20	150	–	–	60	64.1	0.25	72	0.95
21	150	–	–	60	64.1	0.35	42	0.95
22	150	–	–	80	83.7	0.18	94	0.95
23	150	–	–	80	83.7	0.25	85	0.96
24	150	–	–	80	83.7	0.35	52	0.95
25	150	0.3	5	60	64.1	0.18	102	0.97
26	150	0.3	5	60	64.1	0.25	91	0.97
27	150	0.3	5	60	64.1	0.35	62	0.96
28	150	0.3	5	80	83.7	0.18	115	0.96
29	150	0.3	5	80	83.7	0.25	102	0.95
30	150	0.3	5	80	83.7	0.35	75	0.97
	Effect of effective confining pressure							
31	50	0.3	5	40	42.2	0.18	127	0.97
32	50	0.3	5	40	42.2	0.25	93	0.96
33	50	0.3	5	40	42.2	0.35	73	0.97
34	100	0.3	5	40	42.2	0.18	101	0.95
35	100	0.3	5	40	42.2	0.25	87	0.95
36	100	0.3	5	40	42.2	0.35	61	0.95

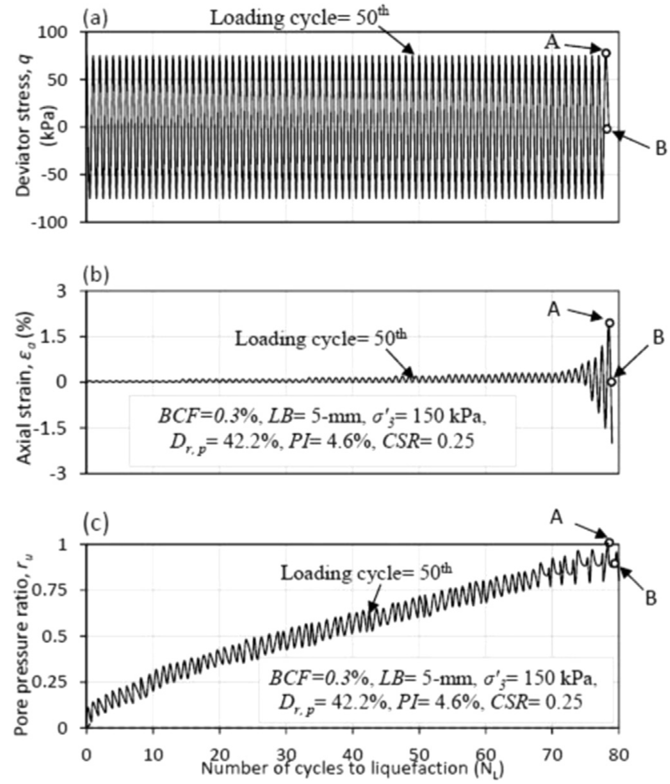

Fig. 3. Typical results of the cyclic triaxial test for a reinforced specimen for *BCF* = 0.3%, *Dr, p* = 42.2%, *CSR* = 0.25, and *σ'3* = 150 kPa. (a) Variation of the deviator stress (*q*) with number of cycles to liquefaction (*NL*); (b) Variation of the axial strain (*εa*) with number of cycles to liquefaction (*NL*); and (c) Variation of the pore pressure ratio (*ru*) with number of cycles to liquefaction (*NL*).

stress induced ± 2% axial strain and complete generation of the excess pore water pressure (r_u) after 79 cycles, which caused a complete liquefaction state for this specimen. Points A and B illustrate the corresponding points at the 79th cycle number in deviatoric stress, axial strain, and pore water pressure ratio graphs. It is seen from Fig. 3(b) that the axial strain (ε_a) development was uniform and very low until the 72nd cycle number, where it increased dramatically to the 79th cycle, and then a total failure occurred. The failure envelope has been touched by the stress state at this point [24]. Also, it is seen from Fig. 3(c) that variation of the pore water pressure ratio with number of cycles to liquefaction (r_u-N_L) in the 79th loading cycle reached one, which indicates a liquefied specimen. It is seen from Figs. 4 and 5 that the effective stress path for the unreinforced and reinforced specimens is decreased, however with a lower rate in reinforced specimens. In fact, the declining rate for the reinforced specimens is lower than the unreinforced specimens since the voids are replaced with the BCF, which causes dissipation of excess pore water pressure [12].

5.2. Effect of BCF contents

The effect of BCF contents on the number of cycles to liquefaction (N_L) for reinforced specimens was presented in Fig. 6. Also, the N_L values for unreinforced specimens were presented to control the improvement, and for ease of comparison. Fig. 6(a) shows the variations of the cyclic stress ratio with the number of cycles to liquefaction (*CSR*-N_L) for unreinforced and reinforced specimens. It is seen that the unreinforced specimens liquefy earlier than the reinforced specimens in all tested CSR values. Also, the results show that the specimens containing 1% BCF liquefy later than the specimens containing 0.5%, and 0.3% BCF. For instance, the unreinforced specimens liquefied at cycle numbers 17, 42, and 60 when tested at CSR values of 0.35, 0.25, and 0.18 respectively. The N_L values improved when the specimens were reinforced with 0.3% BCF. For instance, a cycle number of 33, 79, and 86 was recorded at CSR numbers of 0.35, 0.25, and 0.18 when 0.3% BCF was used in the specimens. An identical trend in a greater range was recorded when the specimens were reinforced with 0.5% BCF as shown in Fig. 6(b). For instance, the specimens liquefied at cycle numbers of 44, 90, and 114 when tested at the CSR values of 0.35, 0.25, and 0.18 respectively. The addition of 1% BCF improved the number of cycles to liquefaction even more. For instance, a cycle number value in the range of 48 ≤ N_L ≤ 137 was recorded at a CSR range value of 0.18 ≤ *CSR* ≤ 0.35. The acquired results in this section is consistent with reported results by [12,25].

5.3. Effect of BCF length (BL)

The effect of the three BCF lengths (*BL*) of 5, 10, and 15-mm on the liquefaction resistance of the silt specimens reinforced with 0.3% BCF is shown in Fig. 7. This figure also shows the liquefaction resistance of the unreinforced (reference) specimens under the same testing conditions. It is seen from the figure that increasing the BCF length caused an increase in the liquefaction strength of the reinforced specimens. The greatest values of the liquefaction numbers belong to the specimens reinforced with 15-mm BCF length and the lowest amounts belong to the specimens reinforced with 5-mm. It is seen from the figure that while the cycle of numbers to liquefaction for unreinforced specimens are 17, 42, and 60 at CSR values of 0.35, 0.25, and 0.18, the addition of

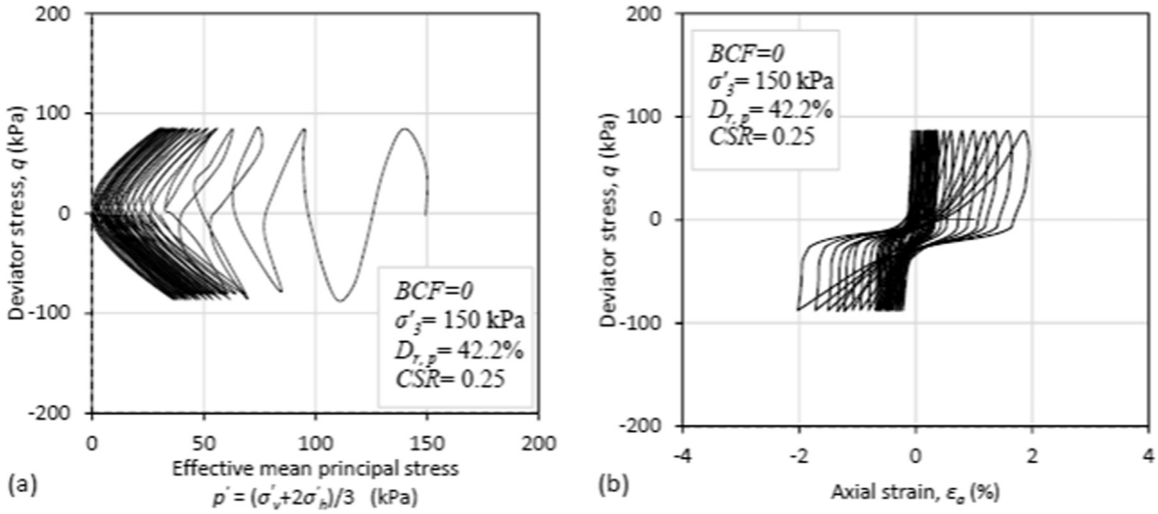

Fig. 4. Typical results of cyclic triaxial test for an unreinforced specimen with *Dr, p* = 42.2%, *CSR* = 0.25, and *σ'3* = 150 kPa (a) Effective stress path; (b) stress-strain relationship (hysteresis loop).

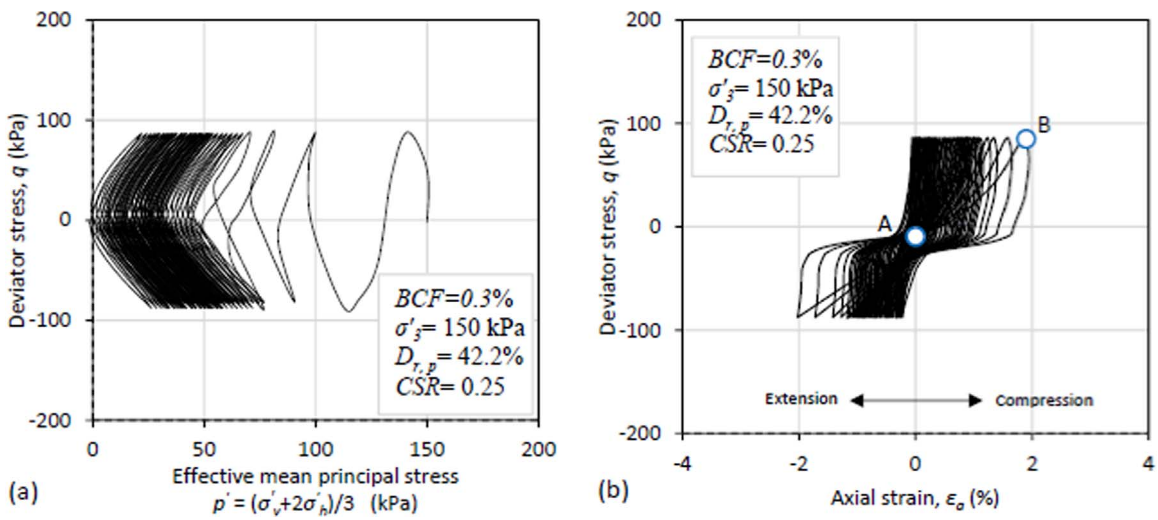

Fig. 5. Typical results of cyclic triaxial test for a reinforced specimen with *BCF* = 0.3%, *Dr, p* = 42.2%, *CSR* = 0.25, and *σ'3* = 150 kPa (a) Effective stress path (b) stress-strain relationship (hysteresis loop).

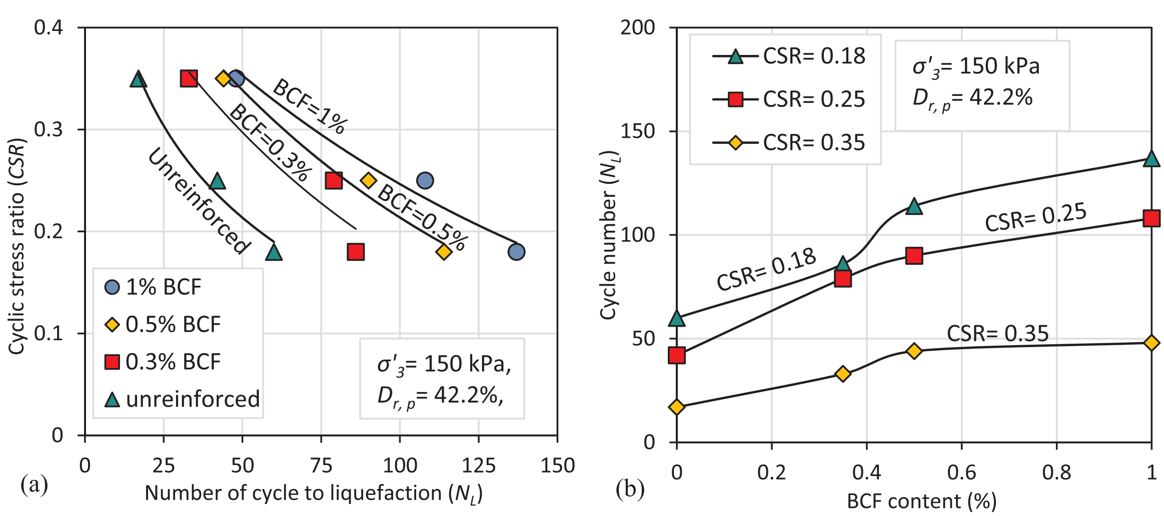

Fig. 6. Effect of BCF contents on liquefaction resistance of reference and reinforced specimens at *Dr, p* = 42.2%, and *σ'3* = 150 kPa (a) Variations of *CSR* with *NL*; (b) Variations of *NL* with BCF contents.

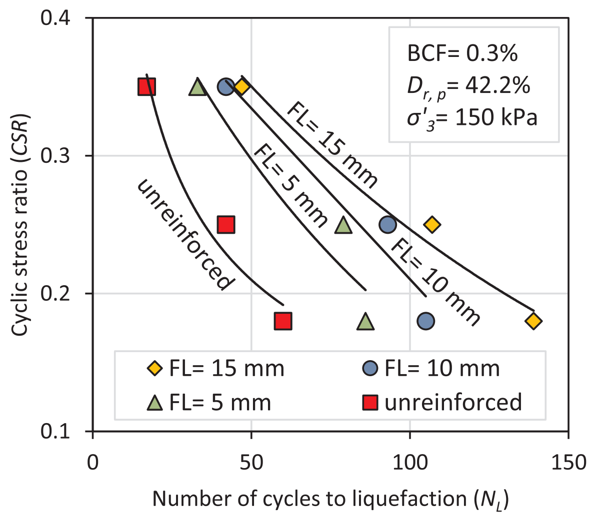

Fig. 7. Effect of BCF length on liquefaction resistance of reference and reinforced specimens for BCF = 0.3%, σ'3 = 150 kPa, and Dr, p = 42.2%.

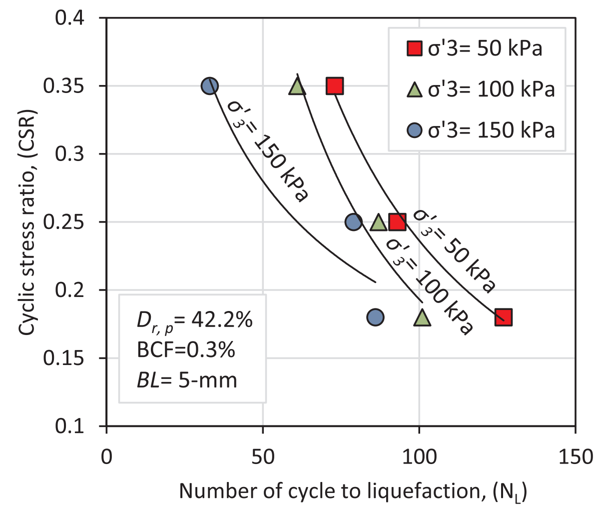

Fig. 9. Effect of effective confining pressure on liquefaction of reinforced specimens when, *BCF* = 0.3%, *BL* = 5-mm, and *Dr, p* = 42.2%.

0.3% BCF content with 5-mm length increased the N_L values to 33, 79, and 86 for the same CSR order. An identical trend but in a greater range was recorded when the reinforcement with the same percentage and a longer BCF was used (i.e., *BCF* = 0.3%, and *BL* = 10-mm), and the N_L values reached 42, 93, and 105 at a CSR value of 0.35, 0.25, and 0.18 respectively. Increasing the BCF length from 10-mm to 15-mm at the same BCF content caused even more increase in N_L values for the specimens tested under the same conditions. For instance, these specimens showed a N_L value of 47, 107, and 139 at CSR values of 0.35, 0.25, and 0.18 respectively. The acquired results in this section is consistent with reported results by [12,25].

5.4. Effect of relative density (D_r)

To investigate effect of relative density *(D_r)* on the liquefaction resistance of the reinforced specimens, a series of cyclic triaxial tests conducted on the unreinforced (i.e., reference tests) and reinforced with 0.3% BCF specimens at three post-consolidation relative densities of 42.2%, 64.1%, and 83.7%. The variations of the cyclic stress ratio (*CSR*) with number of cycles to liquefaction (N_L) for unreinforced and reinforced specimens at different relative densities are shown in Fig. 8. It is seen from the figure that increasing the relative density improved the liquefaction resistance of the specimens. However, this improvement was more pronounced in reinforced specimens. For instance, in unreinforced specimens, the liquefaction resistance of the specimens was in the range of $17 \le N_L \le 60$, $42 \le N_L \le 81$, and $52 \le N_L \le 94$ when the tests were conducted at a post-consolidation relative density ($D_{r,\,p}$) of 42.2%, 64.1%, and 83.7% respectively, whereas, the N_L values in reinforced specimens were in the range of $33 \le N_L \le 86$, $62 \le N_L \le 102$, and $75 \le N_L \le 115$ for a post-consolidation relative density ($D_{r,\,p}$) of 42.2%, 64.1%, and 83.7% respectively.

5.5. Effect of effective confining pressure (σ'_3)

Variations of the number of cycles to liquefaction with CSR for specimens reinforced with 0.3% BCF and tested under effective confining pressure (σ'_3) of 50, 100 and 150 kPa are shown in Fig. 9. It can be seen that the specimens under lower effective confining pressure liquefy later than reinforced specimens at a greater effective confining pressure. For instance, when the tests were conducted under σ'_3 = 50 kPa, a number of cycles to liquefaction in the range of $73 \le N_L \le 127$ at a CSR value of $0.18 \le CSR \le 0.35$ was recorded. Increasing the effective confining pressure from 50 kPa to 100 kPa caused a reduction for N_L in the range of $61 \le N_L \le 101$ at a CSR value of $0.18 \le CSR \le 0.35$. This N_L range value reduced even further to the range of $36 \le N_L \le 86$ at a CSR range value of $0.18 \le CSR \le 0.35$ when the effective

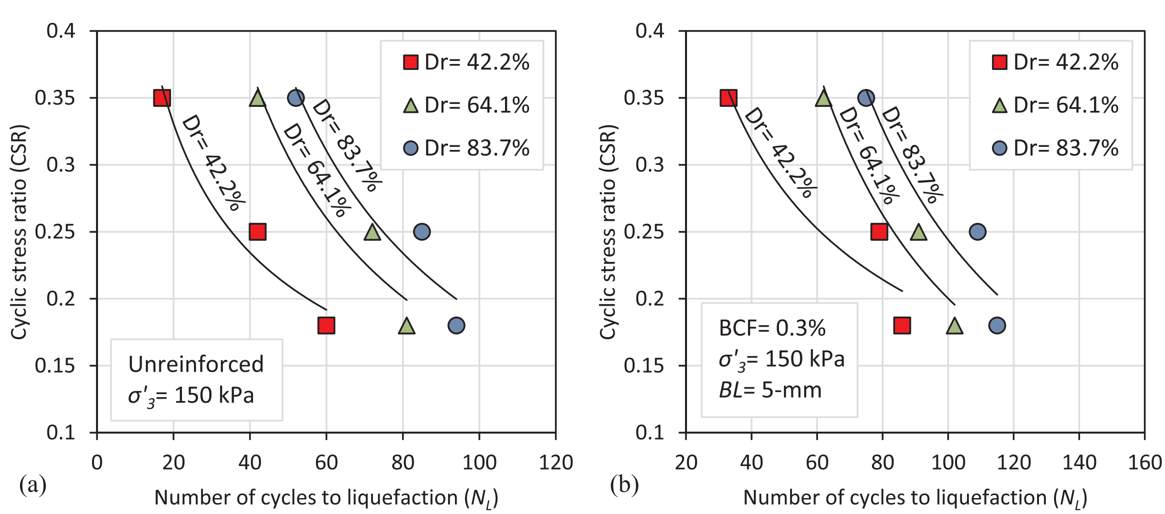

Fig. 8. Effect of relative density on liquefaction resistance of the unreinforced and reinforced specimens at σ'3 = 150 kPa for (a) unreinforced specimen; and (b) reinforced specimens with BCF = 0.3%, and *BL* = 5-mm.

confining pressure increased to 150 kPa. The effect of effective confining pressure on cyclic strength of the soil is known as the effect of K_{σ}, which increases the effective confining pressure caused by suppression of dilatancy [26]. Boominathan and Hari [11] also indicated that the reinforcement is more pronounced at a lower effective confining pressure.

6. Conclusions

This study investigated the effect of BCF reinforcement on low-plasticity silt by performing a total number of 36 cyclic triaxial tests. The effect of three BCF content (i.e., $BCF = 0.3\%$, 0.5% and 1%), three BCF lengths (i.e., $BL = 5$, 10, and 15-mm), three relative densities (i.e., $D_{r,\ p} = 40\%$, 60%, 80%), and three effective confining pressures (i.e., $\sigma'_3 = 50$, 100, and 150 kPa) were investigated, and the results were analysed and compared with the reference tests. To control the repeatability of the results, all the tests were conducted at three cyclic stress ratio values of 0.35, 0.25, and 0.18. According to the presented results, the following conclusions can be drawn from the study:

- Investigations on the effect of BCF contents showed that increasing the BCF percentages in the reinforced specimens increased the liquefaction resistance of the silt.
- Increasing the BCF length from 5-mm to 10 and 15-mm for a given BCF content level increased the liquefaction resistance of the specimens.
- Investigations showed that increasing the relative density in a reinforced specimen is more effective than an unreinforced specimen.
- The results showed that increasing the effective confining pressure for a given reinforced specimen caused a reduction in the liquefaction resistance of the soil. The observed behaviour was attributed to the effect of K_{σ}, for which an increase in effective confining pressure caused suppression of dilatancy, which is consistent with the critical state behaviour of the soil.

References

[1] Wang S, Luna R, Zhao H. Cyclic and post-cyclic shear behavior of low-plasticity silt with varying clay content. Soil Dyn Earthq Eng 2015 31;75:112–20.
[2] Seed HB, Idriss IM, Arango I. Evaluation of liquefaction potential using field performance data. J Geotech Eng 1983;109(3):458–82.
[3] Marto A, Tan CS. Short review on liquefaction susceptibility. Int J Eng Res Appl 2012;2:2115–9.
[4] Bray JD, Sancio RB. Assessment of the liquefaction susceptibility of fine-grained soils. J Geotech Geoenviron Eng 2006;132(9):1165–77.
[5] Polito C. Plasticity based liquefaction criteria. In: Proceedings of the international conferences on recent advances in geotechnical earthquake engineering and soil dynamics. 2001 March; 2001 Paper 25. 〈http://scholarsmine.mst.edu/icrageesd/04icrageesd/session01/25〉.
[6] Prakash S, Puri V, Kumar S. Liquefaction of silts and silt-clay mixtures. Geotech Spec Publ 1998;1:337–48.
[7] Sancio RB, Bray JD, Riemer MF, Durgunoglu T. An assessment of the liquefaction susceptibility of Adapazari silt. In: Proceedings of the 2003 Pacific conference earthquake engineering. New Zealand; 2003 Feb.
[8] Prakash S, Sandoval JA. Liquefaction of low plasticity silts. Soil Dyn Earthq Eng 1992 1;11(7):373–9.
[9] Boulanger RW, Idriss IM. Liquefaction susceptibility criteria for silts and clays. J Geotech Geoenviron Eng 2006;132(11):1413–26.
[10] El Takch A, Sadrekarimi A, El Naggar H. Cyclic resistance and liquefaction behavior of silt and sandy silt soils. Soil Dyn Earthq Eng 2016;83:98–109.
[11] Boominathan A, Hari S. Liquefaction strength of fly ash reinforced with randomly distributed fibers. Soil Dyn Earthq Eng 2002;22(9):1027–33.
[12] Noorzad R, Amini PF. Liquefaction resistance of Babolsar sand reinforced with randomly distributed fibers under cyclic loading. Soil Dyn Earthq Eng 2014;66:281–92.
[13] Vercueil D, Billet P, Cordary D. Study of the liquefaction resistance of a saturated sand reinforced with geosynthetics. Soil Dyn Earthq Eng 1997;16(7):417–25.
[14] Maher MH, Ho YC. Behavior of fiber reinforced cemented sand Under static and cyclic loads. Geotech Test J, GTJODJ 1993;16(3):330–8.
[15] Keramatikerman M, Chegenizadeh A, Nikraz H. Experimental study on effect of fly ash on liquefaction resistance of sand. Soil Dyn Earthq Eng 2017;93:1–6.
[16] ASTM D4221-11. Standard test method for dispersive characteristics of clay soil by double hydrometer. West Conshohocken, PA: ASTM International; 2011http://dx.doi.org.dbgw.lis.curtin.edu.au/10.1520/D4221-11.
[17] ASTM D4318-10e1. Standard test methods for liquid limit, plastic limit, and plasticity index of soils. West Conshohocken, PA: ASTM International; 2010http://dx.doi.org.dbgw.lis.curtin.edu.au/10.1520/D4318.
[18] ASTM D2487-11. Standard practice for classification of soils for engineering purposes (Unified soil classification system). West Conshohocken, PA: ASTM International; 2011. http://dx.doi.org/10.1520/D2487-11.
[19] Bradshaw AS, Baxter CD. Sample preparation of silts for liquefaction testing. Geotech Test J 2007;30(4):1–9. http://dx.doi.org/10.1520/GTJ100206. [ISSN 0149-6115].
[20] Wang S, Luna R, Stephenson RW. A slurry consolidation approach to reconstitute low-plasticity silt specimens for laboratory triaxial testing. Geotech Test J 2011;34(4):1–9. http://dx.doi.org/10.1520/GTJ103529. [ISSN 0149-6115].
[21] Ladd R. Preparing test specimens using undercompaction. Geotech Test J 1978;1(1):16–23.
[22] Vanden Berghe J-F, Holeyman A, Dyvik R. Comparison and modeling of sand behavior under cyclic direct simple shear and cyclic triaxial testing. In: Proceedings of the international conferences on recent advances in geotechnical earthquake engineering and soil dynamics. Paper 34; March 26, 2001.
[23] American Society for Testing and Materials ASTM. Standard test method for load controlled cyclic triaxial strength of soil (D5311-04). Annual book of ASTM standards. Vols. 04–09; 2004.
[24] Karim ME, Alam MJ. Effect of non-plastic silt content on the liquefaction behavior of sand–silt mixture. Soil Dyn Earthq Eng 2014 31;65:142–50.
[25] Diambra A, Ibraim E, Russell AR, Wood DM. Modelling the undrained response of fibre reinforced sands. Soils Found 2011;51(4):625–36.
[26] Seed RB, Harder LF. SPT-based analysis of cyclic pore pressure generation and undrained residual strength. In: Bolton H. Seed memorial symposium proceedings. Vol. 2; 1990. p. 351–76.